



High-birefringence microfiber Sagnac interferometer based humidity sensor



Li-Peng Sun, Jie Li, Long Jin, Yang Ran, Bai-Ou Guan*

Guangdong Provincial Key Laboratory of Optical Fiber Sensing and Communications, Institute of Photonics Technology, Jinan University, Guangzhou 510632, China

ARTICLE INFO

Article history:

Received 6 November 2015

Received in revised form 21 March 2016

Accepted 21 March 2016

Available online 23 March 2016

Keywords:

Humidity sensor

Fiber-optic sensors

Micro-optical devices

ABSTRACT

A relative humidity (RH) sensor based on a microfiber Sagnac loop interferometer is proposed and demonstrated. The sensor is formed by fusion splicing a high-birefringence elliptical microfiber into a fiber loop mirror without any humidity sensitive coating to the structure. Interferometric fringe with visibility of around 30 dB can be achieved in the transmission spectrum due to phase difference between the two polarization modes travelling through the microfiber region. The proposed structure presents high sensitivity up to ~ 201.25 pm/%RH, within an RH range from 30%RH to 90%RH. Moreover, we realize the sensitivity enhancement (up to ~ 422.2 pm/%RH) by inserting a reference Panda fiber into the fiber loop. The sensitivity is two to five times of magnitude higher than the counterparts in the literature. The measured response time is around 60 ms, which is much better than the previously-reported devices.

© 2016 The Authors. Published by Elsevier B.V. This is an open access article under the CC BY-NC-ND license (<http://creativecommons.org/licenses/by-nc-nd/4.0/>).

1. Introduction

The measurement of relative humidity (RH) is required in many fields, such as air conditioning, chemical processing, food processing pharmaceutical and semiconductor industries [1]. In recent years, fiber optic humidity sensors have been studied widely due to their many advantages such as compact size, high sensitivity, good resistance to chemical corrosion, and insusceptibility to electromagnetic interference. Various fiber optic RH sensors have been realized with fiber Bragg gratings (FBGs) [2,3], long period gratings [4,5], photonic crystal fibers [6–8] and interferometers [9–13]. Compared with amplitude based structures, wavelength based sensors can overcome the limitations of power fluctuations and thus have many potential applications, with the help of widespread wavelength interrogation apparatus. However, in a general structure, light is strictly confined in the optical fiber core region, which limits the interaction enhancement between light and the environment quantity. To overcome this problem, one may reduce the cladding region of the structure by polishing or tapering it [14]. Besides, deposition of functionalized coatings having response to external humidity was also proposed [1–9]. However, the surface coating or deposition would make the sensor fabrication process complicated and lower the reliability of the system.

Optical microfiber sensors have received great interest in sensing applications due to their strong evanescent field and flexibility. They bring new opportunities for the realization of highly sensitive fiber optic RH sensors [14]. For example, a microfiber knot sensor can exhibit sensitivity of ~ 12 pm/10%RH [15]. A silica fiber taper interferometer-based RH sensor can exhibit high RH sensitivity of 97.76 pm/%RH, temperature stability of 4.74 pm/°C, and response time of ~ 188 ms, respectively [16]. The response time is in general better than the film-coated sensors.

In this paper, we demonstrate a high sensitivity RH sensor by utilizing a high-birefringence (Hi-Bi) elliptical microfiber Sagnac loop interferometer, without the use of any special coatings. RH sensitivity exhibits two to five times of magnitude enhancement compared to the counterparts in the literature. The response time is better than the previous sensors [1–9].

2. Sensor configuration and principle

Fig. 1 shows the schematic diagram of the humidity sensor based on the Hi-Bi elliptical microfiber Sagnac interferometer. A section of Hi-Bi microfiber that contains two transition regions and a central uniform waist region, together with a Hi-Bi Panda fiber, is fusion spliced into a fiber loop mirror. The microfiber waist has a micrometer size so that light could be extended in the whole silica region. High birefringence of the microfiber is mainly induced by elliptical structure cross section. The polarization states of light can be adjusted by the polarization controllers of PC₁ and PC₂. The Panda

* Corresponding author.

E-mail address: tguanbo@jnu.edu.cn (B.-O. Guan).

fiber is applied to enhance the RH sensitivity of the device. The spectral characteristic is measured by using a broad band light source (BBS) and an optical spectrum analyzer (OSA). Light from the BBS splits into clockwise and counterclockwise beams via 3 dB coupler as it enters the loop. The polarimetric interference fringes can be achieved by the recombination of the counter propagating beams at the coupler. The optical path difference between the polarized light beams is determined by the relative azimuths of the Hi-Bi fibers. The transmission (T) output may be expressed as [17]

$$T = \left[\cos \left(\frac{\pi \Delta n_1 L_1 + \pi \Delta n_2 L_2}{\lambda} \right) \cos \theta_2 \sin (\theta_1 + \theta_3) + \cos \left(\frac{\pi \Delta n_1 L_1 - \pi \Delta n_2 L_2}{\lambda} \right) \sin \theta_2 \cos (\theta_1 + \theta_3) \right]^2 \quad (1)$$

where $\theta_{1\sim 3}$ represent relative polarization angles, Δn_i and L_i ($i = 1, 2$) are the birefringence and the lengths of the microfiber and the Panda fiber, respectively. By tuning the PC₁ state, the azimuthal angle between the fast (slow) axes of the two Hi-Bi fibers can be modified. We can have $\theta_2 = 0^\circ$ or 90° , corresponding to the parallel or perpendicular of the fast (slow) axes between the two birefringent fibers. PC₂ is used to modify the extinction ratio of the interference spectrum. We can show that the fringes are most visible as $\theta_2 = 0^\circ$ or 90° is satisfied, with

$$T = \cos^2 \left[\frac{\pi}{\lambda} (B_1 L_1 \pm B_2 L_2) \right] \quad (2)$$

where “+” and “−” corresponds to the parallel and perpendicular states for the fast (slow) axes between the two Hi-Bi fibers, respectively, $B_i = n_{\text{eff}}^x - n_{\text{eff}}^y$ represents the modal birefringence for the two Hi-Bi fibers, and n_{eff}^x and n_{eff}^y are the mode indices for the x and y polarizations, respectively, with $i = 1, 2$. In principle, RH response of the Hi-Bi microfiber Sagnac interferometer can be attributed to the environmental refractive index change. The index changes induce modification of the microfiber birefringence, so that the interference wavelength shifts. By considering a small variation of RH from the transmission Eq. (1) for Φ to be considered a constant, we obtain

$$S = \frac{d\lambda}{dRH} = \frac{\lambda}{G_1 \pm G_2 (L_2/L_1)} \frac{\partial B_1}{\partial RH} \quad (3)$$

where $G_i = B_i - \lambda \partial B_i / \partial \lambda$ represents the group birefringence of the respective Hi-Bi fibers, with $i = 1, 2$. From Eq. (3), the sensitivity is determined by three parameters: wavelength λ , RH-induced birefringence variation $\partial B_1 / \partial RH$, and relative group birefringence $G_1 \pm G_2 (L_2/L_1)$. Without Panda fiber, we have $S = (\lambda/G_1) \cdot \partial B_1 / \partial RH$. The sensitivity is significantly enhanced in condition of $G_1 \rightarrow 0$. This condition can be achieved by optimizing the profile and the size of the elliptical microfiber, as demonstrated in [18], [19], [20]. With Panda fiber, high sensitivity is achieved in condition of $G_1 \pm G_2 (L_2/L_1) \rightarrow 0$. Such a condition can be obtained by optimizing the relative fiber length, i.e. L_2/L_1 , and tuning the polarization state of PC₁, with $L_2/L_1 \sim G_1/G_2$.

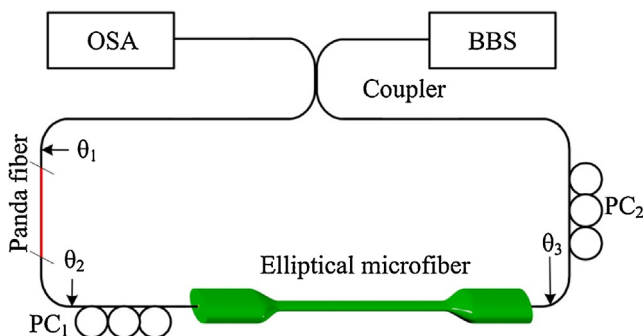


Fig. 1. Schematic diagram of the Hi-Bi elliptical microfiber Sagnac interferometer based RH sensor.

3. Experimentations and discussions

3.1. Fabrication of humidity sensor

As shown in Fig. 1, the sensing is realized due to the interaction between the evanescent mode field of the Hi-Bi elliptic microfiber and external physical quantities. In our experiment, the elliptic profile of the fiber cross section is fabricated by cutting away the part of

the silica cladding on the opposite sides of a standard single-mode fiber. A pulsed CO₂ laser (SYNRAD 48-5) is used for the fabrication. The output laser beam after transmitted through a ZnSe lens has a diameter of $\sim 50 \mu\text{m}$ and power of 17.5 W. When the high-power laser beam is irradiated onto a fiber surface, a dramatic temperature promotion occurs due to the photon absorption effect, resulting in the sputtering of fiber material and the deformation of fiber shape. To obtain the elliptical fiber, we place a standard single-mode fiber perpendicularly to the laser-irradiating direction, as shown in Fig. 2(a). The laser spot scans along the transversal direction of the fiber with a speed of 300 mm/s and a repetition frequency of 5 kHz and then moves along the axial direction with a period of $20 \mu\text{m}$, under the control of a computer. The fiber holders can be rotated by 180° to allow the opposite side of the fiber to be machined. The whole fabrication procedure is monitored by use of a CCD camera. After one-cycle laser milling process, an elliptical

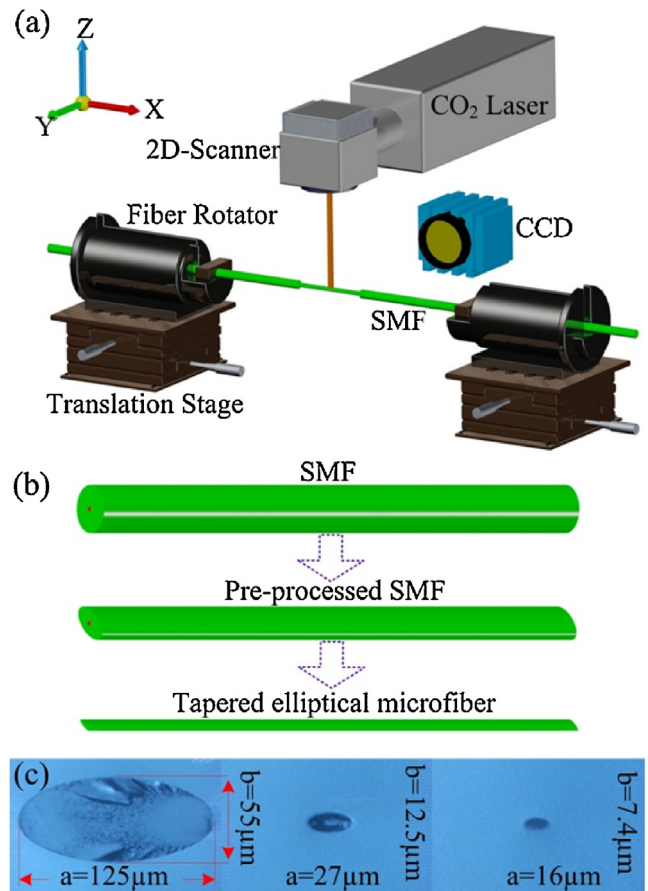


Fig. 2. (a) Schematic of the CO₂-laser-machining system for elliptic fiber fabrication. (b) Described the fabrication process of the elliptical microfiber. (c) Cross-sectional microscope images of elliptical fibers.

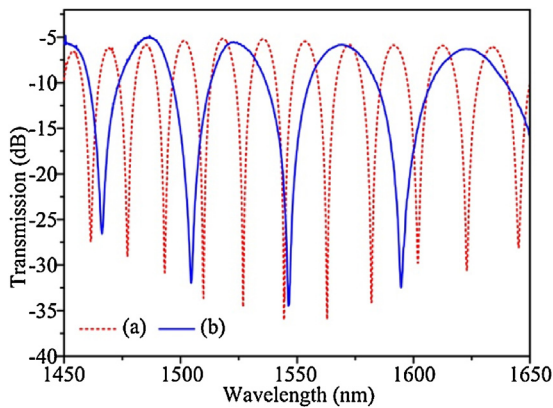


Fig. 3. Transmission spectra of the interferometers with $a=2.17\ \mu\text{m}$, $b\sim 1.09\ \mu\text{m}$, $L_1=8.5\ \text{mm}$, and (a) $L_2=0\ \text{cm}$ and (b) $L_2=14\ \text{cm}$.

fiber can be produced (a and b represent the longer and shorter axes of the ellipse in the cross section of fiber). The length is set to 6 mm. With the increase of CO_2 -laser output power, the fiber ellipticity is improved [20]. For example, at laser power of 13W, an ellipticity of 1.5 is obtained in the fiber and that can be enhanced to 2.5 as the laser power is set to 17.5 W. Then the elliptical fiber is stretched by the use of the flame-heated taper-drawing technique. The cross-sectional fiber shape can be well preserved with optimization of the fiber tapering speed and the heating temperature [19]. The birefringence is determined by the fiber ellipticity with the same tapered size of a . Calculation shows that the birefringences are 5.7×10^{-2} with ellipticity of 2.5 and 1.6×10^{-2} with ellipticity of 1.5 for the microfiber with $a=2\ \mu\text{m}$ at wavelength of 1550 nm.

The used microfiber has parameters of $a=2.17\ \mu\text{m}$, $b\sim 1.09\ \mu\text{m}$, $L_1=8.5\ \text{mm}$, which generates a modal birefringence of $\sim 4.3 \times 10^{-3}$. Fig. 3(a) and (b) record the transmission spectrum of a microfiber-based loop mirror without and with a piece of Panda fiber ($L_2=140\ \text{mm}$), respectively. The fast axes of the elliptical microfiber and the Panda fiber are mutually perpendicular, i.e., $\theta_2=90^\circ$. The transmission spectra both have the fringe visibility of higher than 30 dB and the insertion loss of smaller than 6 dB. Comparison shows that the interferometer exhibits smaller free spectrum range (FSR) with insertion of the Panda fiber, which is consistent with the description in Eq. (2).

3.2. RH sensitivity

The RH sensitivity is measured by placing our structure into an airtight humidity chamber in which the humidity is controlled automatically and monitored with a hygrometer. We first investigate the simple structure without Panda fiber at the room temperature and the atmospheric pressure. When the RH levels are varied from 30%RH to 95%RH with an increment of 5%RH, the interference fringes shift to the longer wavelength almost linearly. We record the dip wavelength shifts by use of an OSA with a resolution of 0.02 nm. Fig. 4(a) illustrates the relationship between the wavelength shift and humidity of the humidity varying from 30%RH to 95%RH. The obtained sensitivity is 201.25 pm/%RH for the dip with wavelength of 1560 nm, 194.09 pm/%RH for the dip with wavelength of 1540 nm. The dip with longer wavelength corresponds to the higher sensitivity. Such sensitivity is much higher than the previously reports [15], [16]. With an increase of humidity, the surrounding refractive index increases, which leads to the decrease of birefringence of the elliptical microfiber, i.e., $\partial B_1/\partial \text{RH} < 0$. Meanwhile, owing to the strong birefringence dispersion of the waveguide, we have $G_1 < 0$. As a result, a positive value of sensitivity S is enabled, corresponding to a redshift of dip wavelengths

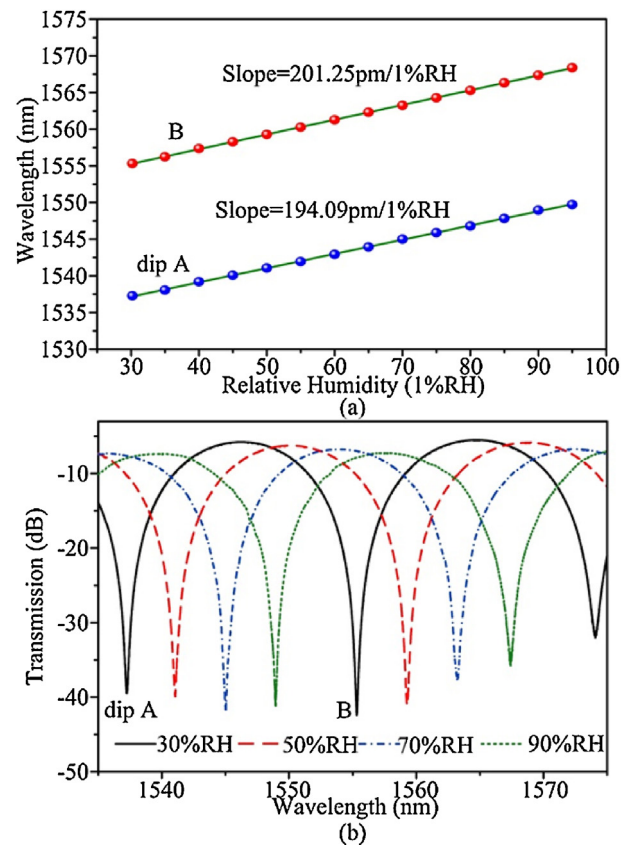


Fig. 4. (a) Measured dip wavelength shift as functions of relative humidity. Dots: measured results; Curve: linear fit. (b) Recorded transmission spectrum of dips at different RH values.

with the increase of RH, as demonstrated in Fig. 4(b). As discussed in Eq. (3), the sensor sensitivity can be further enhanced by optimization of the cross-sectional profile of the elliptical microfiber, which nevertheless may induce a very thin microfiber size and thus a large transmission loss. For improving the sensitivity, an alternative way is proposed by using a reference Hi-Bi Panda fiber as shown in Fig. 1.

3.3. RH sensitivity with Panda fiber as the reference

Fig. 5(a) and (b) show the dip wavelength responses and the transmission spectra, respectively, for the humidity varies from 30%RH to 90%RH after insertion of a Panda fiber into the interferometric fiber loop. The lengths of microfiber and Hi-Bi Panda fiber are 8.5 mm and 140 mm, respectively. By tuning the polarization state of PC_1 , we obtain the maximum sensitivity of 422.2 pm/%RH, which is much higher than that without Panda fiber. The presence of the Panda fiber enhances the RH sensitivity by 1.78 times. The longer wavelength in general presents higher sensitivity.

3.4. Response time

We carry out an investigation of the response time of the sensor by injecting a laser beam into the loop interferometer and then tracing the transmitted light power with an optical power meter. A narrow-line tunable laser (Anritsu, Tunics-Plus) is used in this experiment. The center wavelength of the laser is tuned to the center of the interferometer transmission dip. As shown in Figs. 4 and 5, when the external RH level is slightly changed, the transmitted laser power varies due to the shift of the interferometer fringe. Before investigating the response time, we measure the stability of the input laser and the interferometer under a fixed

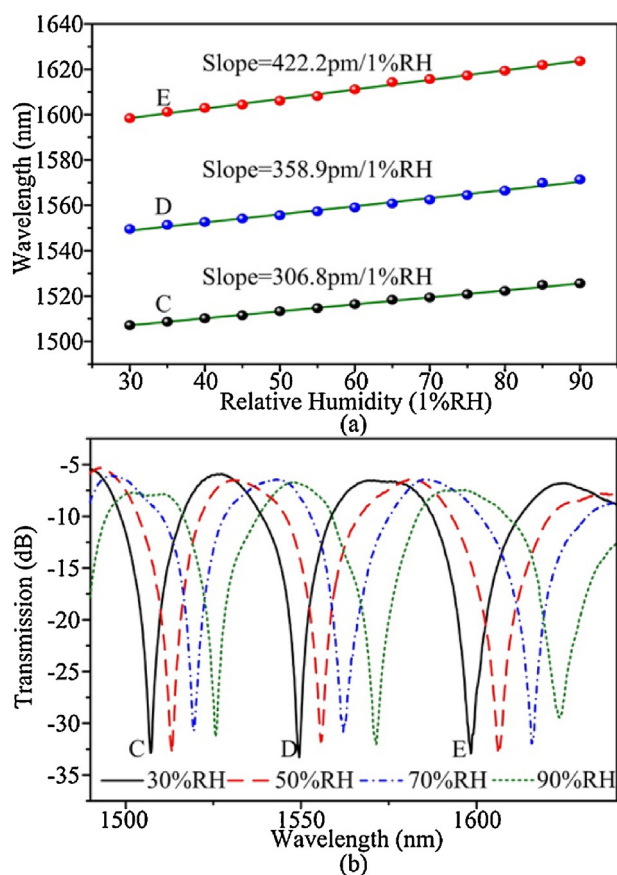


Fig. 5. (a) Measured dip wavelength shift as a function of relative humidity. Dots: Measured results; Curve: Linear fit. (b) Recorded transmission spectrum of dips at different RH levels.

external RH of $\sim 60\%$. The center wavelength of the laser is set to 1550 nm. As shown in Fig. 6(a), their long-term intensity fluctuations are 0.021 dB and 0.024 dB, respectively, showing a relatively good stability of the proposed sensor.

Fig. 6(b) records the variation of the output laser power with change of the external RH. The transmitted laser power increases from -32.742 dBm to -29.051 dBm quickly with the RH varying from 75% to 80%, and vice versa. The measured response time is better than 60 ms, meaning that the response speed of our device is one or two orders of magnitude faster than the conventional counterparts in the literature [1–9]. Such a fast response speed may be attributed to the compactness of the structure and the non-use of functionalized film, which enables a rapid diffusion or evaporation of the water molecules [21]. Our proposed sensor could have potentials in the near real-time analysis of dynamic humidity changes, such as those associated with human breathing events for improvement of health care.

4. Conclusion

In conclusion, we have investigated an optical humidity sensor by utilizing a high-birefringence microfiber Sagnac loop interferometer, without special treatment to the structure. The high sensitivity can be obtained with 201.25 pm/%RH (without Panda fiber) and 422.2 pm/%RH (with Panda fiber), which have been improved by two to five times compared to the counterparts in the literature. Measurement shows that the structure can have a response time of better than 60 ms, suggesting a fast response speed compared to the previous devices.

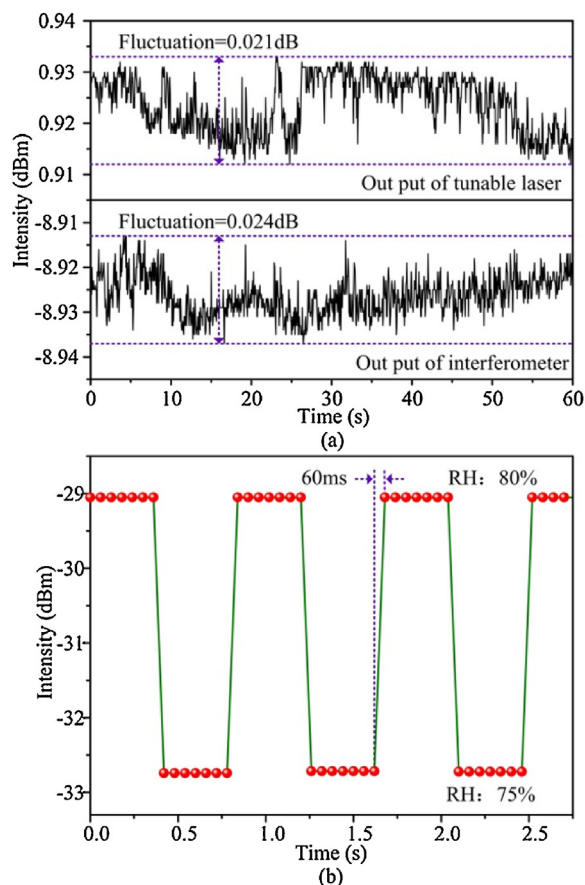


Fig. 6. (a) Recorded intensity variation of the tunable laser and the output from the interferometer. (b) Measured reversible response of the sensor obtained by alternately cycling the surrounding RH between 80% and 75%.

Acknowledgements

This work is supported by the National Science Fund for Distinguished Young Scholars of China (61225023), the National Natural Science Foundation of China (11374129 and 61575083), the Planned Science and Technology Project of Guangzhou (2012J5100028), the Project of Science and Technology New Star of Zhujiang in Guangzhou city (2012J2200062), and the Guangdong Natural Science Foundation (S2013030013302 and 2014A030313364).

References

- [1] T.L. Yeo, T. Sun, K.T.V. Grattan, Fibre-optic sensor technologies for humidity and moisture measure, *Sens. Actuators A* 144 (2008) 280–295.
- [2] T.L. Yeo, T. Sun, K.T.V. Grattan, D. Parry, R. Lade, B.D. Powell, Characterization of a polymer-coated fiber Bragg grating sensor for relative humidity sensing, *Sens. Actuators B* 110 (2005) 148–156.
- [3] P. Kronenberg, P.K. Rastogi, P. Giaccari, H.G. Limberger, Relative humidity sensor with optical fiber Bragg gratings, *Opt. Lett.* 27 (2002) 1385–1387.
- [4] M. Konstantaki, S. Pissadakis, S. Pispas, N. Madamopoulos, N.A. Vainos, Optical fiber long-period grating humidity sensor with poly (ethylene oxide)/cobalt chloride coating, *Appl. Opt.* 45 (2006) 4567–4571.
- [5] T. Venugopalan, T. Sun, K.T.V. Grattan, Long period grating-based humidity sensor for potential structural health monitoring, *Sens. Actuators A* 148 (2008) 57–62.
- [6] J. Mathew, Y. Semenova, G. Farrell, Relative humidity sensor based on an agarose-infiltrated photonic crystal fiber interferometer, *IEEE J. Sel. Top. Quantum* 18 (2012) 1553–1559.
- [7] T. Li, X. Dong, C.C. Chan, K. Ni, S. Zhang, P.P. Shum, Humidity sensor with a PVA-coated photonic crystal fiber interferometer, *IEEE Sens. J.* 13 (2013) 2214–2216.
- [8] W.C. Wong, C.C. Chan, L.H. Chen, T. Li, K.X. Lee, K.C. Leong, Polyvinyl alcohol coated photonic crystal optical fiber sensor for humidity measurement, *Sens. Actuators B* 174 (2012) 563–569.

- [9] P. Hu, X. Dong, K. Ni, L.H. Chen, W.C. Wong, C.C. Chan, Sensitivity-enhanced Michelson interferometric humidity sensor with waist-enlarged fiber bitaper, *Sens. Actuators B* 194 (2014) 180–184.
- [10] C. Zhong, C. Shen, Y. You, J. Chu, X. Zhou, X. Dong, Y. Jin, J. Wang, A polarization-maintaining fiber loop mirror based sensor for liquid refractive index absolute measurement, *Sens. Actuators B* 168 (2012) 360–364.
- [11] W.C. Wong, W. Zhou, C.C. Chan, X. Dong, K.C. Leong, Cavity ringdown refractive index sensor using photonic crystal fiber interferometer, *Sens. Actuators B* 161 (2012) 108–113.
- [12] Y. Geng, X. Li, X. Tan, Y. Deng, Y. Yu, Highly-sensitivity Mach-Zehnder interferometric temperature fiber sensor based on a waist-enlarged fusion bitaper, *IEEE Sens. J.* 11 (2011) 2891–2894.
- [13] J.S. Santos, I.M. Raimundo, C.M. Cordeiro, C.R. Biazoli, C.A. Gouveia, P.A. Jorge, Characterisation of a Nafion Film by optical fibre Fabry-Perot interferometry for humidity sensing, *Sens. Actuators B* 196 (2014) 99–105.
- [14] L.M. Tong, R.R. Gattass, J.B. Ashcom, S.L. He, J.Y. Lou, M.Y. Shen, I. Maxwell, E. Mazur, Subwavelength-diameter silica wires for low-loss optical wave guiding, *Nature* 426 (2003) 816–819.
- [15] Y. Wu, T.H. Zhang, Y.J. Rao, Y. Gong, Miniature interferometric humidity sensors based on silica/polymer microfiber knot resonators, *Sens. Actuators B* 155 (2011) 258–263.
- [16] Y. Tan, L.P. Sun, L. Jin, J. Li, B.O. Guan, Temperature-Insensitive humidity sensor based on a silica fiber taper interferometer, *IEEE Photonic Technol. Lett.* 25 (2013) 2201–2204.
- [17] J. Wang, K. Zheng, J. Peng, L. Liu, J. Li, S. Jian, Theory and experiment of a fiber loop mirror filter of two-stage polarization-maintaining fibers and polarization controllers for multiwavelength fiber ring laser, *Opt. Express* 17 (2009) 10573–10583.
- [18] L.P. Sun, J. Li, Y. Tan, X. Shen, X. Xie, S. Gao, B.O. Guan, Miniature highly-birefringent microfiber loop with extremely-high refractive index sensitivity, *Opt. Express* 20 (2012) 10180–10185.
- [19] J. Li, L.P. Sun, S. Gao, Z. Quan, Y.L. Chang, Y. Ran, L. Jin, B.O. Guan, Ultrasensitive refractive-index sensors based on rectangular silica microfibers, *Opt. Lett.* 36 (2011) 3593–3595.
- [20] L.P. Sun, J. Li, S. Gao, L. Jin, Y. Ran, B.O. Guan, Fabrication of elliptic microfibers with CO₂ laser for high-sensitivity refractive index sensing, *Opt. Lett.* 39 (2014) 3531–3534.
- [21] F.J. Arregui, Y. Liu, I.R. Matias, R.O. Claus, Optical fiber humidity sensor using a nano Fabry-Perot cavity formed by the ionic self-assembly method, *Sens. Actuators B* 59 (1999) 54–59.

Biographies

Li-Peng Sun received the B.S. degree from the Hefei University of Technology, Hefei, China, in 2010. He is currently working toward the Ph.D. degree at the Institute of

Photonics Technology, Jinan University, Guangzhou, China. His research interests include optical fiber devices and fiber optic sensors.

Jie Li received the B.S. degree in applied physics and the M.S. degree in optics from Nankai University, Tianjin, China, in 2000 and 2003, respectively, and the Ph.D. degree in electronic engineering from the City University of Hong Kong, Kowloon, Hong Kong, in 2008. From 2003 to 2004, he was at the Chuangnam Company Ltd., Shenzhen, China. From 2008 to 2009, he was a Postdoctoral Researcher at the Photonics Research Centre and the Department of Electronic and Information Engineering, The Hong Kong Polytechnic University, Kowloon, Hong Kong. Since 2009, he has been with the Institute of Photonics Technology, Jinan University, Guangzhou, China, as an Associate Professor. His current research interests include optical fiber devices, optical fiber sensors, and photonic crystal fibers.

Long Jin received the B.S. degree in applied physics and the Ph.D. degree in fiber optics from Nankai University, Tianjin, China, in 2003 and 2008, respectively. He joined the Department of Electrical Engineering, Hong Kong Polytechnic University, in 2008, as a Research Assistant, where he was also a Postdoctoral Research Fellow. Since 2010, he has been with the Institute of Photonics Technology, Jinan University, Guangzhou, China, as an Associate Professor. He has published more than 50 journals and conference papers. His research interests include fiber optic devices, specialty optical fibers, and photonic sensors.

Yang Ran received the B.S. degree from Dalian University of Technology, Dalian, China, in 2006, and the Ph.D. degree from Jinan University, Guangzhou, China, in 2013. He is currently a lecturer at the Institute of Photonics Technology, Jinan University, Guangzhou, China. His research interests include optical fiber devices & sensors and optical bio-medical sensors.

Bai-Ou Guan received the B.Sc. degree in applied physics from Sichuan University in 1994, and the M.Sc. and Ph.D. degrees in optics from Nankai University in 1997 and 2000, respectively. From 2000 to 2005, he worked in the Hong Kong Polytechnic University, first as a Research Associate, then as a Postdoctoral Research Fellow. From 2005 to 2009, he worked in Dalian University of Technology, Dalian, as a full professor. In 2009 he joined Jinan University, Guangzhou, where he founded the Institute of Photonics Technology. His research interests include optical fiber sensors, biomedical photonic sensing and imaging, microwave photonics, and photonic components for sensing and telecommunication. He has authored and coauthored more than 130 papers in the SCI-indexed journals and presented 30 invited talks at international conferences. He received the Distinguished Young Scientist Grant from Natural Science Foundation of China (NSFC) in 2012.